

Compositional Homogeneity and Electrical Properties of Lead Magnesium Niobate Titanate Single Crystals Grown by a Modified Bridgman Technique

To cite this article: Haosu Luo *et al* 2000 *Jpn. J. Appl. Phys.* **39** 5581

View the [article online](#) for updates and enhancements.

Related content

- [Growth of \$\text{Pb}\(\text{Zn}_{1/3}\text{Nb}_{2/3}\)_{0.94}\text{Ti}_{0.06}\text{O}_3\$ Single Crystals Directly from Melt](#)
Bijun Fang, Haosu Luo, Haiqing Xu *et al.*
- [Growth of Single Crystals of High-Curie-Temperature \$\text{Pb}\(\text{In}_{1/2}\text{Nb}_{1/2}\)\text{O}_3\$ - \$\text{Pb}\(\text{Mg}_{1/3}\text{Nb}_{2/3}\)\text{O}_3\$ - \$\text{PbTiO}_3\$ Ternary Systems near Morphotropic Phase Boundary](#)
Yasuharu Hosono, Yohachi Yamashita, Hideya Sakamoto *et al.*
- [Top-Seeded Solution Growth of \$\text{Pb}\(\text{In}_{1/2}\text{Nb}_{1/2}\)\(\text{Mg}_{1/3}\text{Nb}_{2/3}\)\text{TiO}_3\$ Single Crystals](#)
Tomoaki Karaki, Maki Nakamoto, Yoichi Sumiyoshi *et al.*

Recent citations

- [Depth dependant element analysis of \$\text{PbMg}_{1/3}\text{Nb}_{2/3}\text{O}_3\$ using muonic x-rays](#)
K L Brown *et al*
- [Multi-functional piezoelectric/magnetostrictive laminated composite for AC and DC magnetic detection](#)
Meng Yao *et al*
- [A polarized micro-Raman study of a \$0.65\text{PbMg}_{1/3}\text{Nb}_{2/3}\text{O}_3\$ - \$0.35\text{PbTiO}_3\$ single crystal](#)
Zhang Li-Yan *et al*

Compositional Homogeneity and Electrical Properties of Lead Magnesium Niobate Titanate Single Crystals Grown by a Modified Bridgman Technique

Haosu LUO*, Guisheng XU, Haiqing XU, Pingchu WANG and Zhiwen YIN

Laboratory of Functional Inorganic Materials, Shanghai Institute of Ceramics, Chinese Academy of Sciences, Shanghai 201800, China

(Received April 24, 2000; accepted for publication June 22, 2000)

Relaxor ferroelectric single crystals $\text{Pb}(\text{Mg}_{1/3}\text{Nb}_{2/3})_{1-x}\text{Ti}_x\text{O}_3$ (PMNT 100(1-x)/100x) were grown directly from melt by a modified Bridgman technique. The segregation during the growth of PMNT single crystals was studied by means of differential thermal analysis (TGA), thermogravimetric analysis (DTA), X-ray diffraction (XRD) and X-ray fluorescence analyzer (XRFA). The results show that PbTiO_3 content increases throughout the crystal growth. The segregation coefficient is about 0.95 during the growth of PMNT 76/24 directly from melt. Therefore, the electric properties of PMNT single crystals vary even in the same boule. It was demonstrated that the homogeneity of PMNT single crystals can be improved by optimizing growth parameters, but it cannot be eliminated because of the effect of segregation during the crystal growth. We have recently improved the growth process of the modified Bridgman technique to increase the homogeneity of the crystals. Good-quality single crystals with a boule size of more than $\phi 40 \times 80$ mm or $30 \times 30 \times 1$ mm plates have been achieved. For PMNT 67/33 crystals, their coupling factors are $k_{33} \approx 94\%$ for the longitudinal mode, $k'_{33} \approx 86\%$ for the beam mode, and $k_t \approx 62\%$ for the thickness mode, and they have the piezoelectric constant $d_{33} = 1500\text{--}3000$ pC/N, and dielectric constant $\epsilon_{33}/\epsilon_0 = 3500\text{--}5500$.

KEYWORDS: relaxor, crystal growth, lead magnesium niobate titanate, phase diagram, segregation, homogeneity, domain, electromechanical coupling factor

1. Introduction

Relaxor ferroelectric $\text{Pb}(\text{Mg}_{1/3}\text{Nb}_{2/3})\text{O}_3$ [PMN] ceramics have been attracting much attention since the 1960s. The most interesting properties of PMN are its high dielectric constant and diffuse phase transition. In recent years it was found that solid solution $(1-x)\text{Pb}(\text{Mg}_{1/3}\text{Nb}_{2/3})\text{O}_3\text{--}x\text{PbTiO}_3$ [PMNT] single crystals have a high dielectric constant, a high piezoelectric constant and a large electromechanical coupling factor.¹⁾ For example, PMNT 67/33 single crystals have the ultrahigh piezoelectric constant $d_{33} \sim 2500$ pC/N, and the electromechanical coupling factor $k_{33} \sim 94\%$. The PMNT single crystal is a new piezocrystal that is a promising material for next generation ultrasonic transducers for medical echo and undersea applications.

PMNT single crystals are usually grown by a flux method.²⁾ However, it is difficult to grow large high-quality PMNT due to their complex composition and high evaporation rate of PbO at high temperatures. By studying the relation and stability of the PMN-PT binary system by differential thermal analysis (TGA), thermogravimetric analysis (DTA) and X-ray diffraction (XRD), we found that the phase of the PMN-PT solid solution is unstable beyond 1250°C ; however, the perovskite phase can be grown directly from PMN-PT melt in an isolated system. We developed a new modified Bridgman technique to grow PMNT single crystals.^{3,4)} After much effort in optimizing the growth process,^{5,6)} high-quality PMNT single crystals have been grown with the boule size of 40 mm in diameter and 80 mm in length.

In this paper, we will report our recent studies on the growth and characterization of relaxor ferroelectric PMNT single crystals.

2. Crystal Growth

Ferroelectric PMNT single crystals were grown by the modified Bridgman technique. Raw powders of PbO , MgO , Nb_2O_5 and TiO_2 with purity of more than 99.99% were used

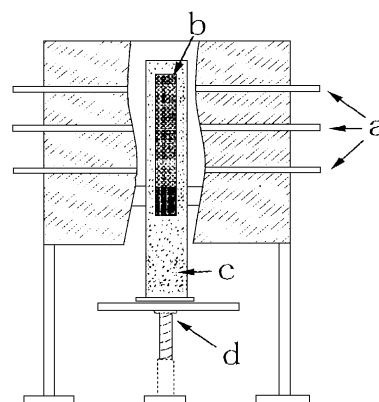


Fig. 1. Schematic diagram of the Bridgman furnace for the growth of PMNT single crystals. (a) MoSi_2 resistance (b) Pt crucible (c) Al_2O_3 powder (d) Drop-down mechanism.

as the starting compounds. The powders were mixed in the range of $(1-x)\text{PMN-}x\text{PT}$, $x: 0.2\text{--}0.4$. PMNT single crystals were grown in sealed platinum crucibles to prevent the evaporation of PbO at high temperatures. The seed crystals were used along the $\langle 001 \rangle$ or $\langle 111 \rangle$ direction for the growth.

The highest furnace temperature is more than 1380°C , and the temperature gradient is about $40\text{--}100^\circ\text{C}/\text{cm}$ at the solid-liquid interface. The furnace temperature was regulated using a proportional integral differential (PID) controller. After soaking for approximately 10 h, the crucible was dropped at the rate of 0.1 to 1.0 mm/h. At the end of the growth process, the furnace temperature was cooled at the rate of $25^\circ\text{C}/\text{h}$ to room temperature.

PMNT single crystals are usually grown with the size of approximately $\phi 40 \times 80$ mm at present. The PMNT single crystals plates are light yellow in color after mirror polishing.

3. Segregation

3.1 Phase diagram

The thermal properties of PMNT single crystals were investigated by DTA and TGA. For the binary system of the $(1-x)\text{PMN-}x\text{PT}$ solid solution, it is difficult to determine

*E-mail address: hsluo@public3.sta.net.cn

the phase diagram accurately at high temperatures only by DTA measurement, because PMNT single crystals are unstable in air above 1250°C. However, several melting points were measured by DTA to evaluate the phase diagram of $(1-x)$ PMN- x PT in an isolated system. The melting points are 1320°C for PMN, 1296°C for PMNT 70/30, 1288°C for PMNT 65/35, and 1284°C for PMNT 60/40. The schematic phase diagram of the $(1-x)$ PMN- x PT binary system at high temperatures in an isolated system is suggested as in Fig. 2.

From Fig. 2, it is evident that the segregation coefficient $k = C_S/C_L$ is less than 1. While PMNT single crystals are grown directly from melt with a low growth rate, the PbTiO_3 content at the initial part of the boule will be less than that in the melt. This conclusion was confirmed during the growth of PMNT from melt by the modified Bridgman method. The PbTiO_3 content in a PMNT solid-solution boule increases with distance from the seed crystal, where the PbTiO_3 content at the ending region is larger than that at the initial region.

3.2 Segregation and phases

The lattice structures of PMNT 67/33 and PMNT 64/36 single crystals were investigated by X-ray diffraction in different regions of two boules, where the composition of the starting compounds is on both sides of the morphotropic phase boundary (MPB). The composition of MPB for the PMN-PT binary system is usually considered as

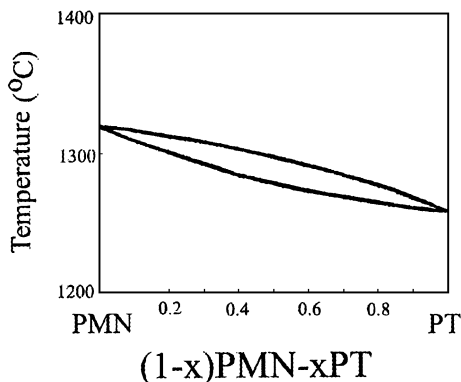


Fig. 2. Schematic of phase diagram of $(1-x)$ PMN- x PT in an isolated system.

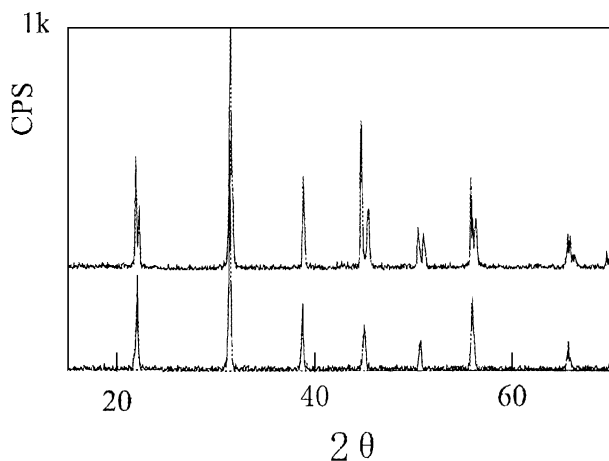


Fig. 3. XRD patterns for the initial part (a) and ending parts (b) in a PMNT 67/33 boule.

$x = 0.33-0.35$. The results show that the phase of $(1-x)$ PMN- x PT solid solution in the two boules was changed from rhombohedral to tetragonal, where x increases across the MPB during the crystal growth.

XRD patterns (Fig. 3) show that the composition of the PMNT 67/33 boule varied with the distance from the seed crystal. The rhombohedral phase appeared at the initial part of the boule; however, the peaks of the rhombohedral phase gradually split into peaks of tetragonal phase during the ending part. For example, the first peak $(100)_R$ split into the peaks $(100)_{TR}$ and $(001)_{TR}$. This result shows that the PbTiO_3 content increases during the growth due to segregation according to the phase diagram of $(1-x)$ PMN- x PT at low temperatures.

Another example is a PMNT boule grown directly from melt with the composition of PMNT 64/36, where $x = 0.36$ is larger than x at MPB. If PMNT 64/36 was a complete congruently melting compound, the initial part of the PMNT single crystal would be tetragonal phase at room temperature. However, XRD patterns show that the PbTiO_3 content in the single crystal is in the range of the rhombohedral phase, which is less than the PbTiO_3 content in the melt of PMNT 64/36. This result indicates that due to segregation, the initial part of the PMNT 64/36 single crystal is rhombohedral phase at room temperature. The peaks of the rhombohedral phase were split at the ending part in the boule, which show that the phase transition was induced by the increase in PbTiO_3 content.

3.3 Segregation and fluctuation of electric properties

Because there is segregation during the growth of solid solution PMNT single crystals, variation of the composition will lead to the fluctuation of the electric properties of PMNT plates such as the dielectric constant, piezoelectric constant and electromechanical coupling factor. For a boule of PMNT 67/33 of 80 mm in length, the dielectric constants usually vary in the range of 3500 to 5500 for the poled (001) plates with the Cr-Au electrode of $1\ \mu\text{m}$ thickness. Of course, all these fluctuations result not only from variation of the composition, but also from other factors such domain configurations, lattice imperfections and space charges.

The variation of Curie temperature T_C is shown in Fig. 4 for the same samples as in Fig. 3. T_C is 144.4°C at the initial part of the boule (Fig. 4(a)), and 172.8°C at the ending part of the boule (Fig. 4(b)). The temperature of the phase transition from the rhombohedral to the tetragonal phase changes from 46.2°C to 88.6°C.

In a PMNT 67/33 boule, the piezoelectric constant d_{33} usually varies in the range of 1500 to 3000 pC/N, and the electromechanical coupling factor k_t varies in the range of 0.58 to 0.62.

3.4 Segregation coefficient

PMNT single crystals are light yellow in color after their surface has been polished. The polished PMNT plates usually appear to be uniform from their color; however, the composition varied with the plates cut from the different regions of a boule can be measured directly using an X-ray fluorescence analyzer (XRFA). For a single crystal grown from the initial composition of PMNT 76/24, the boule composition, which varies with distance from the seed crystal, was measured by XRFA, and listed in Table I. Because of segregation, the PbTiO_3 content increases with distance from the seed crystal.

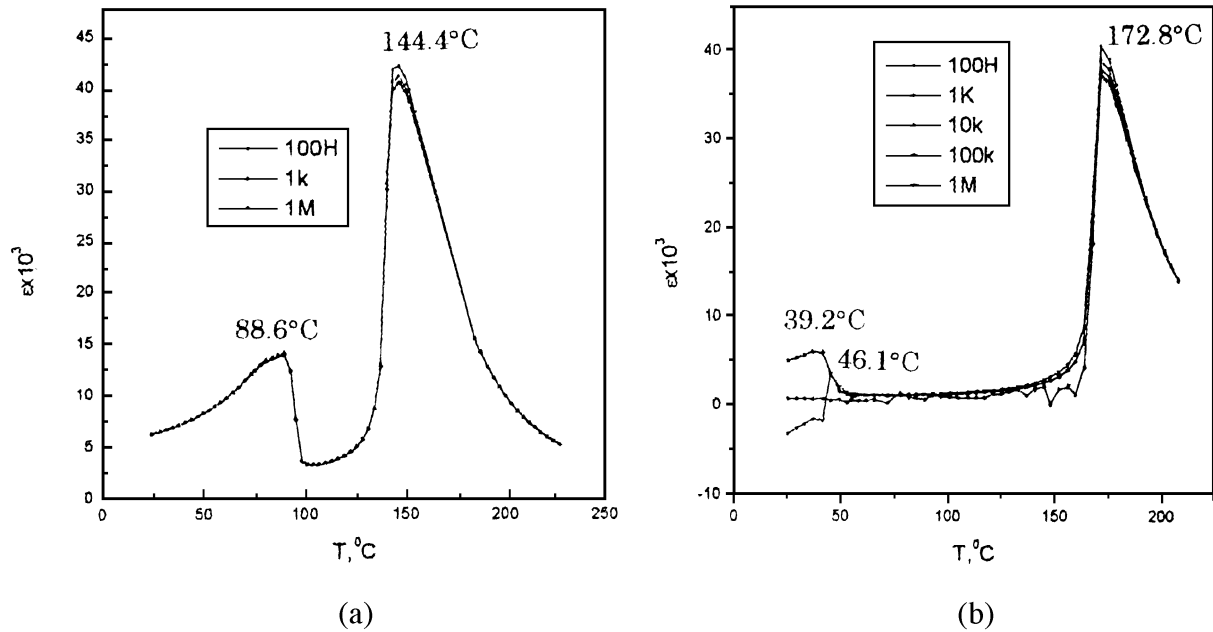


Fig. 4. Temperature frequency dependence of the dielectric constant of poled plates cut from the initial and ending parts of the PMNT 67/33 single-crystal boule shown in Fig. 3 (measured upon heating).

Table I. Composition of a boule varied with distance d (mm) from the seed crystal grown from PMNT 76/24 melt (XRFA results: x mole%).

D(mm)	PbO	MgO	Nb ₂ O ₅	TiO ₂	Mg _{1/3} Nb _{2/3}	x
0.0–0.1	102.38	24.33	25.87	22.12	75.3	0.2276
20.0–20.1	100.85	25.59	25.73	22.73	76.64	0.2288
30.0–30.1	101.42	25.17	25.47	22.62	75.96	0.2295
Stoichiometry	100	25.33	25.33	24	75.99	0.2400

From Table I, the segregation coefficient k for PbTiO₃ content during the growth of PMNT 76/24 in our growth process can be calculated as

$$k = C_S/C_L(\infty) = 0.95, \quad (1)$$

where $C_L(\infty)$ is the PbTiO₃ mole concentration at a significant distance from the growth boundary. While PMNT single crystal is grown directly from melt, the segregation coefficient for PbTiO₃ is 0.95. There PMNT single crystal can be considered a near congruently melting compound only at short distances from the seed crystal.

For the segregation coefficient $k = C_S/C_L(\infty)$ in relation to the growth rate and the boundary layer thickness, there is the well-known Burton, Prim and Slichter equation,

$$k = \frac{k^*}{k^* + (1 - k^*) \exp(-v\delta_m/D)}, \quad (2)$$

where $k^* = C_S/C_L(0)$, D is the mass diffusion coefficient, δ_m is the thickness of the boundary layer adjacent to the interface, and v is the steady velocity of the solid-liquid interface during the crystal growth.

From eq. (2) we see that the effective segregation occurs at low growth rates. Because the PbTiO₃ content increases in the boundary layer during the crystal growth, the boundary layer becomes unstable when the PbTiO₃ content crosses the concentration threshold, where the constitutional supercooling takes place. The patterns of dendrite growth of PMNT

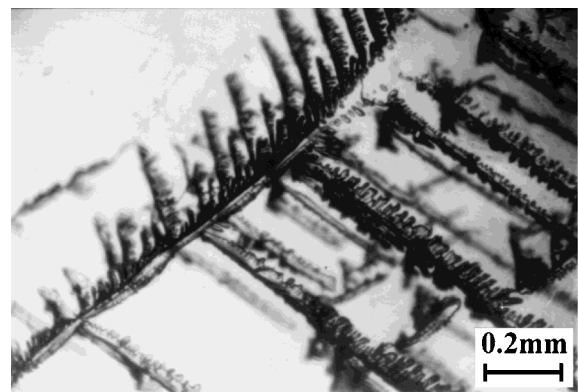


Fig. 5. Dendrite growth of PMNT single crystal due to constitutional supercooling.

(Fig. 5) were determined for the unstable solid-liquid interface due to constitutional supercooling.

4. Domain and Phase Transition

The domain configurations in PMNT single crystals were observed using a cross-polarized light microscope and a scanning electron acoustic microscope (SEAM).

The domains in PMNT single crystals near the MPB have straight wide strips, of which dark and bright ones are alternately arranged, as revealed by the cross-polarized light

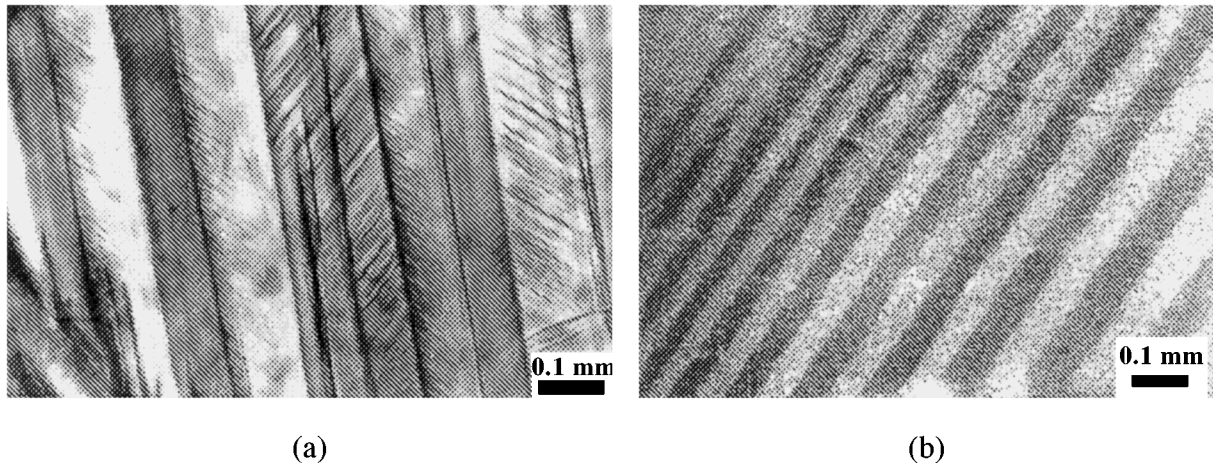


Fig. 6. Domain structure, showing bright and dark strips under a cross-polarized light microscope (a) and SEAM (b).

microscope or SEAM as illustrated in Fig. 6. The non- 180° domain walls are along (110) not only in the rhombohedral phase but also in the tetragonal phase. Figure 6(a) shows that there are substructures (micrometer order in width) in most coarse domain strips under transmitted light for PMNT 67/33. The broadest width of the coarse strips is of millimeter order. Figure 6(a) also shows a 71° (or 109°) domain on the {001} plate, illustrating two groups of right-angled (110) domain walls for composition PMNT 67/33 under transmitted light observation.

It was observed that there is a superposition of domains in PMNT 67/33 single crystals. As shown in Fig. 6, small strips of non- 180° domains exist within the large strip of domains, which result from the formation of different nucleations during the phase transition from the PA to the FE phase. The intervals between domains varied from less than 0.01 mm to more than 0.1 mm, due to the different rates of plane phase boundary movement though the PMNT single crystal while the phase transition occurs.

It was found that PMNT single crystal is difficult to pole in a single domain. Many small non- 180° domain strips remained even after poling the PMNT plate along the [001] direction. So it is suggested that the polarization orientations in four directions [111], $[\bar{1}\bar{1}\bar{1}]$, $[\bar{1}\bar{1}1]$, $[1\bar{1}\bar{1}]$ have equal probability in multidomains. Statistically, the multidomain configurations in PMNT 67/33 single crystals have 4 mm symmetry after poling along the [001] direction, although PMNT 67/33 single crystal has R3m local symmetry in its lattice.

Two phase transitions; PA \rightarrow FE (m3m \rightarrow 4mm) and FE \rightarrow FE (4mm \rightarrow 3m), occurs in PMNT crystals with the composition near the MPB while the temperature decreases from about 190°C to room temperature. Figure 7 shows that these two phase transitions occurs while temperature decreased across 155°C from the cubic to the tetragonal phase, and across 70°C from the tetragonal to the rhombohedral phase.

The dielectric properties of PMNT single crystals sensitively depend on the PbTiO_3 content, which varies in a boule due to segregation. The PbTiO_3 content in a boule of PMNT 67/33 varies from rhombohedral phase at the initial part to tetragonal phase at the ending part, which is a typical example of composition-induced phase transition.

Dielectric constants under free stress for PMNT 67/33 sin-

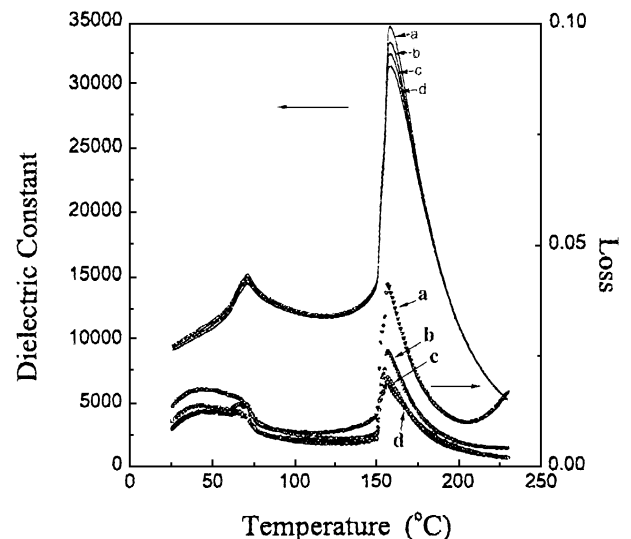


Fig. 7. Temperature and frequency dependence of the dielectric constant of PMNT 67/33 single crystals at (a) 100 Hz (b) 1 kHz (c) 10 kHz (d) 100 kHz.

gle crystals usually vary from 3500 to 5500. One of the main reasons for this is the variation of composition during the growth of PMNT single crystals.

It was found that the Curie temperature varied with PbTiO_3 content in PMNT single crystals. For plates sliced from different regions of an as-grown PMNT 67/33 single crystal, the Curie temperature varies in the range of 145 to 175°C due to the effect of segregation. Temperature T_{TR} of the phase transition from 4mm to R3m is very sensitive to PbTiO_3 content. For plates sliced from different regions of an as-grown PMNT 67/33 single crystal, the temperature T_{TR} can vary from 40°C to 90°C .

5. Characterization

We have optimized the growth process with the modified Bridgman technique to enable the fabrication of large high-quality PMNT single crystals by studying the formation of lattice imperfections, the phase transition and the domain configuration of PMNT single crystals. At present, good-quality single crystals of sizes greater than $\phi 40 \times 80$ mm or $30 \times 30 \times 1$ mm plates have been achieved. For PMNT

Table II. Beam mode of PMNT 67/33 single crystal orientated (001) face.

Measured values									
	Density	Thickness(mm)		Width	Length	f_s	Y_{max}	f_p	Z_{max}
	g/cm ³	Bare	Elect.	mm	mm	MHz	S	MHz	Ω
No. 1	8.01	1.039	1.040	0.530	14.54	0.970	0.0122	1.790	109200
No. 2	8.01	1.039	1.040	0.530	14.54	1.042	0.0109	1.756	54475.5
Calculated parameters									
	V^L	Z_S	k'_{33}	C_0	ϵ^S	ϵ^T	Q_m	Q_e	Q_{tot}
	km/s	$\times 10^6$ kg/m ² s		nF					
No. 1	3.720	29.79	0.864	0.069	1053	4143	140.3	29.8	111.9
No. 2	3.649	29.23	0.832	0.089	1357	4407	95.4	17.1	62.7

Table III. Thickness mode of PMNT 67/33 single crystals orientated (001) face.

Measured values									
	Density	Thickness(mm)		Width	Length	f_s	Y_{max}	f_p	Z_{max}
	g/cm ³	Bare	Elect.	mm	mm	MHz	S	MHz	Ω
Mean	8.01	1.0611	1.0625	14.883	17.06	1.783	0.546	2.182	1108.0
Std Dev	0.00	0.0323	0.0314	1.558	1.65	0.055	0.171	0.063	230.8
Std Dev(%)	0.00	3.0441	2.9560	10.469	9.67	3.081	31.3	2.878	20.83
Calculated parameters									
	V^L	Z_S	k_t	C_0	ϵ^S	ϵ^T	Q_m	Q_e	Q_{tot}
	km/s	$\times 10^6$ kg/m ² s		nF					
Mean	4.627	37.52	0.616	5.550	227	4233	269.0	10.3	46.8
Std Dev	0.036	0.29	0.007	0.899	284	460	47.3	2.8	17.4
Std Dev(%)	0.78	0.78	1.16	16.20	10.8	10.9	17.6	27.2	37.2

67/33 crystals, the coupling factors are $k_{33} \approx 94\%$ for the longitudinal mode, $k'_{33} \approx 86\%$ for the beam mode, and $k_t \approx 62\%$ for the thickness mode, and they have piezoelectric constant $d_{33} = 1500\text{--}3000$ pC/N, and a dielectric constant $\epsilon_{33}/\epsilon_0 = 3500\text{--}5500$.

In Table II and Table III, C_0 and ϵ^S are the clamped capacitance and the clamped dielectric constant, respectively, obtained from the best fit data from the impedance curve at high frequency. As evident in Table III, the inhomogeneity due to lattice imperfections and segregation at crystal growth leads to the variation of the dielectric and piezoelectric properties of PMNT single crystals. It is demonstrated by our study that the homogeneity of PMNT single crystals can be improved by optimizing the growth process, but it cannot be eliminated because of segregation.

The results of our study on crystal growth show that relaxor ferroelectric PMNT single crystal is a suitable material for application in ultrasonic transducers and high strain actuators.

6. Conclusions

Segregation will occur during the growth of PMNT single crystals directly from melt, which leads to the increase of the PbTiO₃ content during the crystal growth. While PMNT single crystals were grown with compositions on both sides of the MPB, the composition of a boule will gradually be changed from in the range of rhombohedral phase at the initial part to tetragonal phase at the ending part.

The properties of PMNT single crystals vary even within the same boule. The inhomogeneity of PMNT single crystals

mainly resulted from the variation of the composition and multidomains will lead to the variation of dielectric and piezoelectric properties. Our results demonstrate that the homogeneity of PMNT single crystals can be improved by optimizing the growth process, but it cannot be eliminated because of the effect of segregation during the growth of solid solution PMNT single crystals.

We have improved the growth process involving the modified Bridgman technique to increase the homogeneity of the fabricated crystals. Good-quality single crystals with boule sizes greater than $\phi 40 \times 80$ mm or $30 \times 30 \times 1$ mm plates have been achieved.

Acknowledgements

This work was supported by the National Sciences Foundation of China (Grant Nos. 59995520 and 59872048), the Chinese Academy of Sciences (Grant No. KY951-A1-205-03), the Shanghai Municipal Government (Grant Nos. 98JC14017 and 99XD14024) and the General Electric Company of USA.

- 1) S.-E. Park and T. R. Shrout: IEEE Trans. Ultrason. Ferroelectr. & Freq. Control **44** (1997) 1140.
- 2) M. Dong and Z.-G. Ye: J. Cryst. Growth **209** (2000) 81.
- 3) Z. Yin, H. Luo, P. Wang and G. Xu: Ferroelectric **299** (1999) 207.
- 4) H. Luo, G. Xu, P. Wang and Z. Yin: Ferroelectric **231** (1999) 97.
- 5) G. Xu, H. Luo, W. Zhong, Z. Yin, H. Xu, Z. Qi and K. Liu: Sci. China (Series E) **42** (1999) 541.
- 6) G. Xu, H. Luo, P. Wang, H. Xu and Z. Yin: Chin. Sci. Bull. **45** (2000) 491.